Third International Conference on Sustainable Construction Materials and Technologies http://www.claisse.info/Proceedings.htm

Observation for Internal Cracks of Concrete Affected by Alkali-Silica Reaction and Its Compressive Failure Behavior

Tomohiro Miki[1,*], Yudai Miyagawa[2] and Koichiro Mastutani[2]

[1]*Associate Professor, Department of Civil Engineering, Kobe University, Japan*
[2]*Graduate student, Department of Civil Engineering, Kobe University, Japan*
[*]*1-1 Rokkodai, Nada, Kobe 657-8501, Japan, mikitomo@port.kobe-u.ac.jp*

ABSTRACT

This study presents an investigation to evaluate crack conditions of concrete and its relation to mechanical characteristics of the cracked concrete that is damaged due to alkali-silica reaction (ASR). At first, we have visually observed on-surface and internal cracks of the ASR damaged concrete. Furthermore, uniaxial compressive tests were carried out in order to reveal the relationships between the pattern of ASR crack and compressive failure behavior. By the observation of the internal cracks, the possibility that state of the internal ASR crack could be estimated by surface crack information was indicated. On the other hand, according to the result of the compression test, it was confirmed that the behavior of crack opening in the concrete under compression differed in terms of the width, length, shape of vertical ASR induced cracks and the restriction at the specimens end so that the compressive strength was variable.

Keywords: alkali silica reaction, internal crack, compressive stress-strain relationship, strain distribution, image analysis

1. INTRODUCTION

Alkali silica reaction (ASR) is classified as a chemical reaction between hydroxyl ions in the pore water within the concrete matrix and certain forms of silica. This reaction could lead to volume expansion of concrete and then the significant expansion results in a crack of the concrete. The concrete damaged due to ASR in which cracks occur has different mechanical properties to the sound concrete. The reduction of the elastic modulus of concrete is remarkably observed according to the expansion due to the ASR. On the other hand, the compressive strength of ASR-damaged concrete slightly decreases even if the expansion proceeds. The previous research (Kubo, et al. 2006) indicates, however, that the compressive strength of ASR damaged concrete decreases to about 60% with the expansion of 5000μ. There is a room for an argument on the influence of the ASR induced crack on the mechanical properties of this concrete. Furthermore, when the performance of ASR-damaged concrete structure is evaluated, not only the position and width of the crack, but also irregularities of maltiple phenomenon shold be considered. Since the ASR induced cracks influence the cracks that occur under the external loading, the fundamental research

on the mechanical properties of the ASR damaged concrete are necessary. The aim of this study is to evaluate crack condition that is defined by indexes using crack width, its direction and distribution density of the ASR induced cracks. Futhermore, the the performance concrete is evaluated based on these indexes. In addition to these examination, we carried out a compression test in order to evaluate the performance of the ASR damaged concrete in terms of failure behavior

2. OUTLINES OF EXPERIMENT

2.1 Specimens

The tested specimens were 100 x 100 x 200 mm prisms. Eleven specimens were prepared in this experiment. **Table 1** shows the mix proportion of concrete. The specimen that is one after three-point bending test (Miki et al. 2013) was used. After three-point bending test, each end of the ruptured specimen was polished to make a flat surface of specimens by using a diamond cutter. Therefore, four prism specimens were created from one beam specimen. They were used in observation of internal cracks and in the compression test. Of these specimens, two specimens were used in the observation of internal crack, and nine were in the compression test. Note that the specimens in the observation of internal crack are defined as No.1 to No.2 and the specimens in the compression test are defined as No.3 to No.11.

2.2 Observation of internal cracks

The internal condition of ASR-induced crack was observed by polishing the surface of the specimen and by photographing the polished surface. The specimens No.1 and No.2 were used in this experiment. The observation was performed on both side of 100 x 200 mm rectangular plane. The two surfaces are defined as side A and B, respectively. The target surface was polished around 2 mm by using a polishing machine and abrasive (granularity F100), and the surface was recorded by a scanner (resolution 1600dpi). The process was repeated until polishing designated amount. Here, the crack width and shape could not be measured exactly due to chipping of the crack edge when the specimens were polished without any processing. Therefore, for specimen No.2, we have fixed the crack by injecting low viscosity epoxy resin inside the crack.

2.3 Compression test

The loading setup in the experiment is illustrated in **Figure 1.** This test was carried out on Specimens No.3-11. Loading scenario was set as three series: ①cyclic loading in the post-peak region (with the friction at the specimen ends in the horizontal direction), ②cyclic loading in the post-peak region (without the friction at the specimen ends in the horizontal direction), ③cyclic loading in the pre-peak region. By comparing the results of the series ①

Table 1. Mix proportion of the concrete

G_{max}	slump	W/C	Air	s/a	(kg/m^3)							
(mm)	(cm)	%	%	%	W	C	Sn	Sr	Gn	Gr	NaCl	Agent
20	18	63	5.0	48	181	287	422	432	466	475	12.4	575 ml

Sn: no-reactive fine aggregate, Sr: reactive fine aggregates,
Gn: no-reactive aggregate, Gr: reactive aggregate

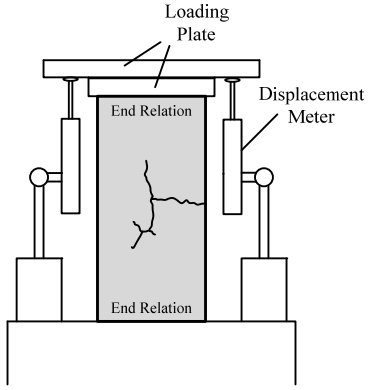

Figure 1. Loading setup

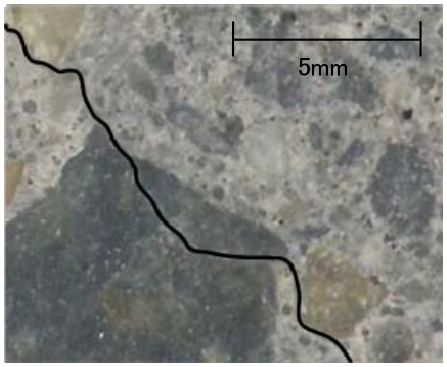

Figure 2. Crack pass through around aggregate

and ②, the difference in fracture behavior with the strength of end restraint is considered. By the result of series ③, the state of the ASR induced crack is observed when the concrete is subjected to a low number cyclic loading. The load, axial deformation and surface strain were measured in the test. During the cyclic loading in the pre-peak region, number of loading was set as 100-200 times between 150kN and 250kN loads. The surface of specimens was photographed during loading and then the image analysis (Miki and Hayashi, 2010, Miki and Nishino, 2010) was performed using these digital images to determine the principal strain distribution on the concrete surface.

3. OBSERVATION OF INTERNAL CRACKS OF CONCRETE

3.1 Crack patterns

In this observation, the specimen No.1 was polished until 8 mm depth from both ends while No2 was polished until 10mm. As an example of the result, the image for the side A of No.2 was shown in **Figure 2**. The figure shows that the ASR induced crack of the specimen in this observation occurs passing through the boundary between matrix and aggregate to be sewing between aggregates. It was also observed that few cracks penetrated to the aggregate.

3.2 Relations of the width to depth of ASR induced cracks

Figure 3 shows photograph and crack pattern of polished surface in the side A of No.2. From figures for 6mm and 10 mm polishing from the surface, only a crack pattern is shown to make it easy to confirm crack width. The ASR induced cracks observed on the concrete surface were classified in three ranges of crack width: less than 0.1 mm, between 0.1 mm and 0.2 mm, and larger than 0.2 mm. In each range, the total value of the crack width was calculated. It was confirmed that the internal ASR crack was compatible with according to the position and shape of the crack. Herein, these internal cracks were classified again according to the crack width of surface, and the total of crack length was calculated in each crack width range. The results for the both sides A and B of specimen No.2 are shown in **Figures 4 and 5**. The results of the observation indicate that the cracks having more than 0.1 mm width were observed to depth more than 8 mm or 10 mm in most cases. On the other hand, the existing depth of cracks having less than 0.1 mm width were mostly less than 8 mm or 10 mm. This indicates that the crack having less than 0.1 mm width occurs only in an outer thin layer (cover) of the concrete. In order to evaluate the ASR induced crack, not

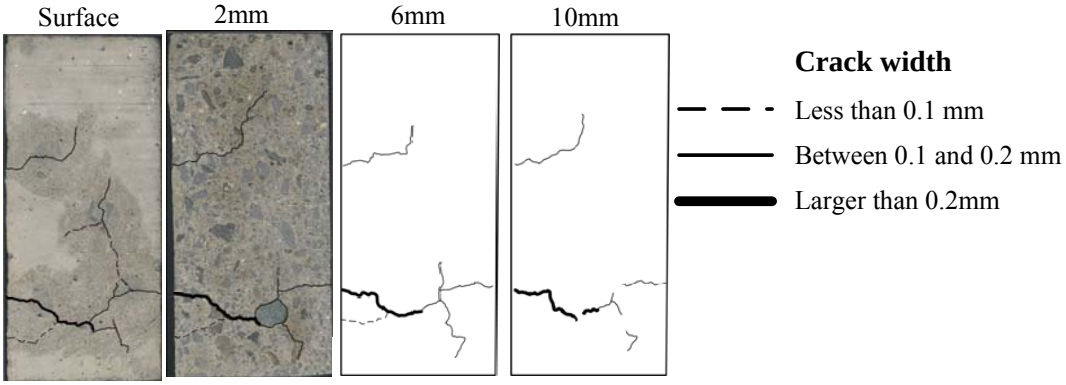

Figure 3. Patterns of internal cracks

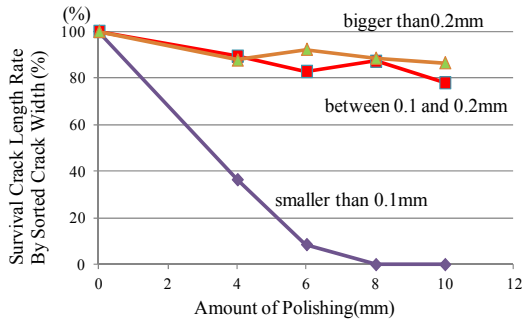

Figure 4. Relations of crack width and depth (side A of No.2)

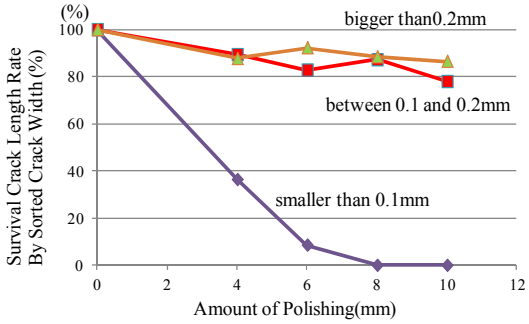

Figure 5. Relations of crack width and depth (side B of No.2)

only the crack width but also the depth from the concrete surface should be investigated since the crack depth varies according to the size of the crack width.

4. RESULTS AND DISCUSSION FOR COMPRESSION TESTS

4.1 Cyclic loading in the post-peak region (with friction at the ends of specimen)

4.1.1 Stress-strain relationships

The cyclic loading was performed in the experiment in which the load on the specimen is released when the stress level reached the maximum until load level decreases to 0.5 kN, and then after reloading the load is released again when the stress increment became zero. The above loading cycles were repeated during the post-peak region. Here, the influence of cyclic loading on the stress-strain relationship might be small since the number of the cyclic loading was set as one.

Figure 6 shows the stress-strain relationships of No.3 to No.6 obtained from the compression test. This figure shows the envelope curves in which the maximums of each stress in the cyclic stress-strain curve are linked. Hereafter we discuss on these stress-strain relationships obtained from loading test. The maximum compressive stress (compressive strength) of the each specimen was found to be different. The cause of maximum stress degradation was investigated using the image analysis to specimens which show the largest or smallest maximum stress, No.4 and No.6.

4.1.2 Distribution of maximum principal strain

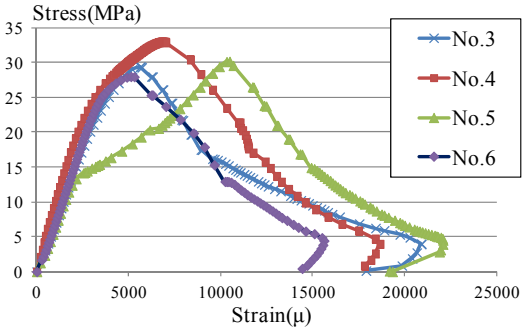

Figure 6. Stress-strain relation (with end friction)

Figure 7 shows distribution of maximum principal strain of No.4 and No.6 and ASR crack patterns, respectively. For both specimens, large tensile strain occurs around vertical ASR induced crack (the region surrounded with a broken line) under compressive loading. Particularly, at around maximum load the large tensile strain occurred exceed to strain of 20000μ. This is because of the large opening of vertical ASR crack under loading. On the other hand, as for the specimen No.4, remarkable tensile strain does not occur during loading. The opening of vertical ASR-induced crack which occurred in the center of the specimen did not increase. This is due to the distribution of width and shape of ASR crack so that the width of the ASR crack is smaller than No.6 and the vertical ASR-induced crack occurs discontinuously within the direction of loading. In addition, for these specimens, the vertical ASR crack affects on the compression failure since the vertical crack opens at peak load. From the above result, the maximum compressive stresses of these specimens differ from each other because of the difference of the width, length and shape of the vertical ASR cracks.

4.2. Cyclic loading in the post-peak region (without friction at the ends of specimen)

4.2.1 Stress-strain relationship

Figure 8 shows the stress-strain relationships of No.7 to No.9. The compressive strength decreases about 30% in the comparison with the case in which the friction at each end of specimen is applied. The comparison of the specimen No. 7 that shows the largest maximum compression stress to the No. 9 showing the smallest stress leads the following discussion.

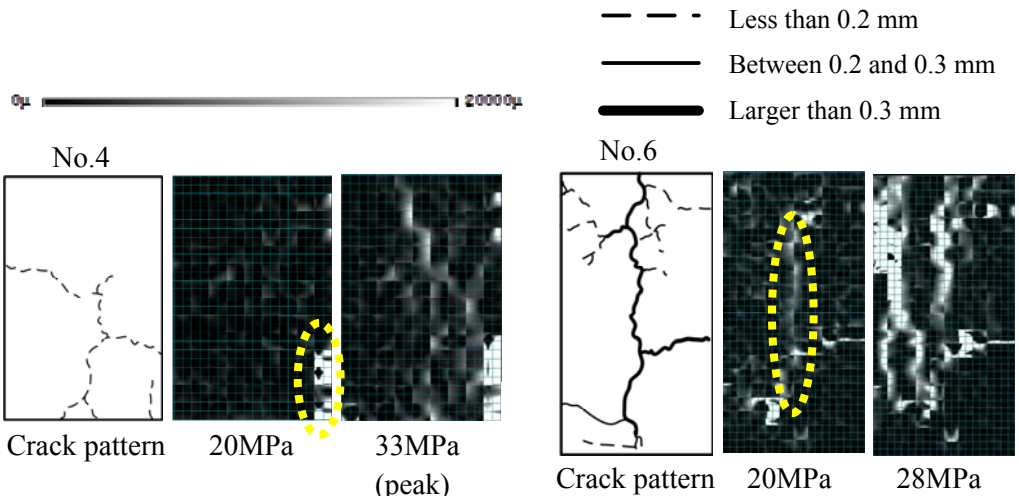

Figure 7. Distribution of maximum principal strain (No.4 and No.6)

4.2.2 Distribution of maximum principal strain

Figure 9 shows distribution of maximum principal strain of No.7 and No.9 and ASR-induced crack patterns, respectively. For both specimens, large tensile strain occurs around the vertical ASR crack in the stress state of 13MPa. These two specimens showed different behavior in a stress state more than 13MPa. For the specimen No.7, the tensile strain which occurred around the vertical ASR crack became larger generally and reached the peak load. On the other hand, as for No.9, the tensile strain that is higher than 20000μ progressed from the upper part. The specimen No.7 showed the behavior that the vertical ASR crack opened overall while the behavior of No.9 showed that the vertical ASR crack opened as splitting from the upper part. The cause of showing different behaviour is that ASR cracks occurred in the vertical direction linearly on No. 9, whereas the shape of cracks on No.7 was that the crack of slant direction continues. In other words, the vertical ASR crack was easier to open and affect on the strength degradation significantly compared to cracks of the slant direction. As mentioned before, the observation for the surface and internal cracks indicates that the crack depth varies according to the size of the crack width. In this research, the ASR induced crack having less than the width of 0.1 mm occurs only in an outer thin covering layer of the concrete. The further challenge which is needed to evaluate the performance of ASR damaged concrete is to accumulate more information on the internal cracks in the concrete mass, especially on the three dimensional distribution of the crack.

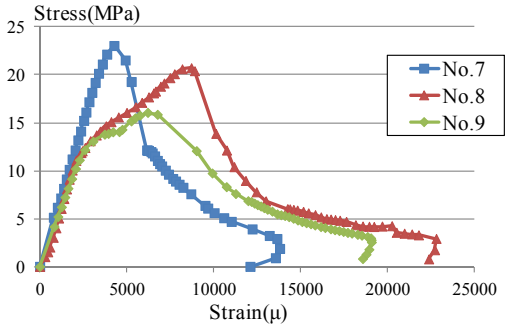

Figure 8. Stress-strain relation (without end friction)

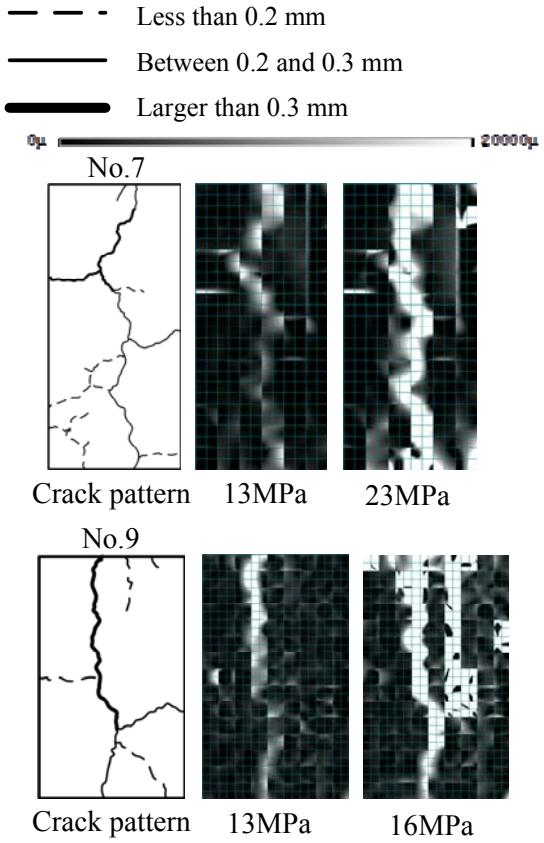

Figure 9. Distribution of maximum principal strain (No.7 and No.9)

4.3 Cyclic loading in the pre-peak region

4.3.1 Stress-strain relationship

Specimens No.10 and No.11 were used in this test where the horizontal friction in their ends was removed. **Figure 10** shows stress-strain relationship of No.10. The cycle load was set

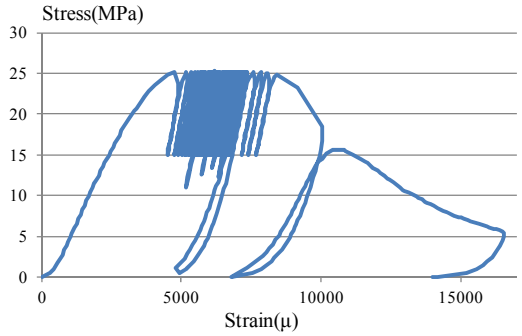

Figure 10. Stress-strain relation (No. 10)

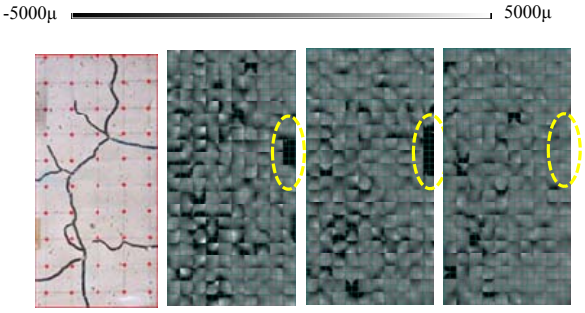

Figure 11. Distribution of minimum principal strain

between 150kN to 250kN. In the cyclic test, specimen No.10 was failed during 54th cycle loading.

4.3.2 Distribution of minimum principal strain

Figure 11 shows distribution of minimum principal stain which is obtained by the image analysis for the specimen of No.10. The strain distributions between upper and lower loads during the first, 26th and 53th are shown in this figure. Here, the strain was calculated from the deformation due to the stress when the specimen is subjected to the maximum load based on the deformation according to the minimum load during each loading cycle. The results in the figure indicate that the compressive strain that indicates the crack closure already occurred around ASR induced crack at the first cycle loading. In addition, it is found that the compressive strain have increased according to the increase of the number of the loading cycles (e.g. the domain surround with a dotted line in **Figure 11**). However, the compressive strain disappeared at the 53th loading cycle which means ASR induced crack remained close at the minimum load in this cycle. This behavior might results in the increase in the axial strain when the number of loading cycle increases. Finally the concrete failed in compression when the ASR induced crack was closed due to the repeated cyclic loading.

5. CONCLISIONS

The conclusions obtained in the present study are drawn as follows:

1) The internal cracks due to the ASR were visually observed in terms of polishing the surface of the concrete. The results of the observation in this study indicate that the crack having less than 0.1mm width occurs only in an outer thin layer (cover) of the concrete.

2) The results of uniaxial compressive loading test show that the maximum compressive stresses of these specimens differ from each other because of the difference of the width, length and shape of the vertical ASR cracks.

3) The results of repeated cyclic loading test indicate that the compressive strain that indicates the crack closure already occurred around ASR crack at the first cycle loading. This compressive strain has accumulated with the increase in the number of the loading cycles. At ultimate states, however, the closure of the ASR induced crack occurred under the compressive cyclic loading.

REFERENCES

Kubo, Y., Ueda, T., Kuroda, T and Nomura, N. (2006), "Influence of ASR expansion on mechanical properties of concrete."*J. of Japan Concrete Institute*, **28**(1), 1691-1696.

Miki, T. and Hayashi, D. (2010). "Measurement of the Strain Distribution of Concrete Subjected to Localized Compression by Using Image Correlation Method." *Memoirs of Const. Eng. Research Institute Foundation*, **52**, 53-60.

Miki, T. and Nishino, Y. (2010). "Experimental Study on Compressive Failure Features of Concrete Cracked Due to Alkali-Silica Reaction." *Proc. of the Conc. Struc. Scenarios*, JSMS **10**, 187-192.

Miki, T., Matsutani, K. and Miyagawa, Y. (2013). "Evaluation of Crack Propagation in ASR Damaged Concrete Based on Image Analysis." *Proc. of 8th Int. Conf. on Frac. Mech. of Conc. and Conc. Struc.* **8**.